Temperature-dependent mechanical-resonance frequencies and damping in ensembles of gallium nitride nanowires

J. R. Montague, K. A. Bertness, N. A. Sanford, V. M. Bright, and C. T. Rogers

---

Articles you may be interested in

Low-frequency noise in gallium nitride nanowire mechanical resonators
Appl. Phys. Lett. **101**, 233115 (2012); 10.1063/1.4769445

High- Q GaN nanowire resonators and oscillators
Appl. Phys. Lett. **91**, 203117 (2007); 10.1063/1.2815747

Diameter dependent transport properties of gallium nitride nanowire field effect transistors
Appl. Phys. Lett. **90**, 043104 (2007); 10.1063/1.2434153

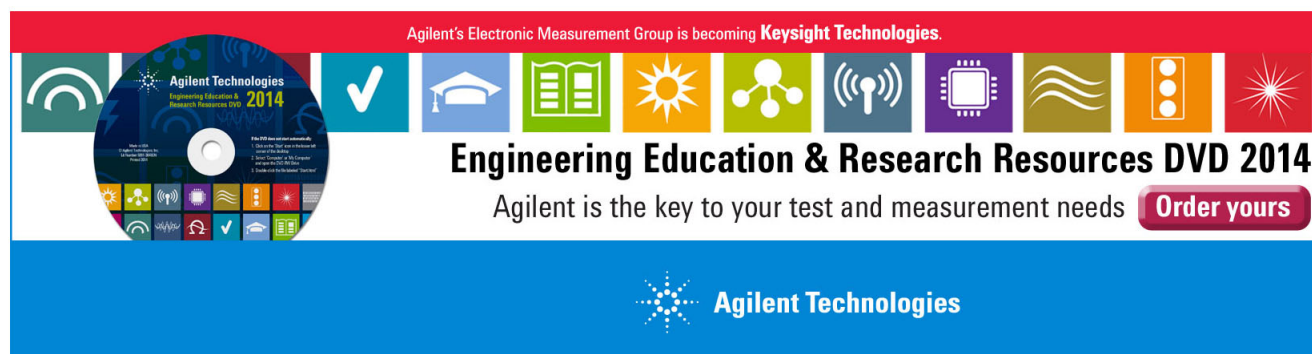High performance thin film bulk acoustic resonator covered with carbon nanotubes
Appl. Phys. Lett. **89**, 143122 (2006); 10.1063/1.2358838

Low-temperature synthesis of silica-enhanced gallium nitride nanowires on silicon substrate
J. Vac. Sci. Technol. A **24**, 1635 (2006); 10.1116/1.2174016

Temperature-dependent mechanical-resonance frequencies and damping in ensembles of gallium nitride nanowires

J. R. Montague,[1,2,a)] K. A. Bertness,[3] N. A. Sanford,[3] V. M. Bright,[4] and C. T. Rogers[1]

[1]*Department of Physics, University of Colorado, Boulder, Colorado 80309, USA*
[2]*DARPA Center for Integrated Micro/Nano-Electromechanical Transducers (iMINT), University of Colorado, Boulder, Colorado 80309, USA*
[3]*National Institute of Standards and Technology, Boulder, Colorado 80305, USA*
[4]*Department of Mechanical Engineering, University of Colorado, Boulder, Colorado 80309, USA*

We have measured singly clamped cantilever mechanical-resonances in ensembles of as-grown gallium nitride nanowires (GaN NWs), from 12 K to 320 K. Resonance frequencies are approximately linearly dependent on temperature near 300 K with relative shifts of 40 ± 20 ppm/K, consistent with temperature-dependent elastic moduli. Below 100 K, we find that some GaN NWs have mechanical quality factors well above 400 000, at mechanical resonance frequencies near 1 MHz. We also observe a correlation between increased amplitude of dissipation and increased temperature dependence of resonance frequencies. The microwave homodyne detection technique we use is simple, allows for the investigation of as-grown or processed NWs, and is sensitive enough to observe the thermal motion of individual NWs while providing for the simultaneous measurement of large ensembles of NW mechanical resonances. © 2012 American Institute of Physics. [http://dx.doi.org/10.1063/1.4761946]

Nanoscale mechanical resonators with high mechanical quality factors, Q (defined as the ratio of resonance frequency to resonance full-width at half-maximum power), and small mass have been shown to be sensitive detectors of motion,[1] force,[2] and mass.[3] Furthermore, as the dimensions of these extremely small, solid-state systems continue to decrease, there exists a growing need to understand how bulk mechanical properties such as elastic moduli and dissipation may be influenced by surface effects and structural details. Gallium nitride nanowires (GaN NWs) have been observed to provide significantly lower mechanical dissipation than that in other untensioned, strain-free nanowire systems[4,5] and thus offer an interesting opportunity to study the sources of dissipation and variations within an ensemble. To better investigate the range of variation that may exist in these mass-produced small systems, we report the results of a systematic study of the mechanical properties of an ensemble of GaN NWs.

The c-axis GaN NWs studied in this work are grown by a molecular beam epitaxial (MBE) process on silicon substrates.[6] Typical NWs from this study are 15 μm in length along the c-axis, have diameters on the order of 100 nm—as shown in Figure 1—and have Young's modulus near 300 GPa. Individual GaN NW resonators have previously been studied by use of electron beam,[4,7] piezoresistive,[8] and individual capacitive[9] measurements. In the as-grown, singly clamped beam geometry studied here, typical room-temperature resonance frequencies and Q factors are, respectively, near 1 MHz and over 10^4.

Our NW ensemble measurement scheme uses capacitive coupling to a microwave homodyne reflectometry system (typically operating near 3 GHz), shown schematically in

Figure 1. Such a system has the important advantages of no direct, physical contact with the resonators, and no processing required beyond NW growth. In this work, the as-grown NW ensemble acts as an array of parallel capacitors with respect to the common sensing electrode (CSE). The CSE is fabricated from high-frequency, thermally stable, printed circuit board laminate using standard lithographic processes. The physical deflections of the NWs modulate the impedance of a microwave tank circuit, its associated resonance frequency, and, subsequently, the reflected microwave power. The NW sample is fixed atop a lead-zirconate-titanate piezoelectric actuator (PZT), which is driven by a white-noise signal with frequency-independent spectral density below 10 MHz. The NW substrate is mechanically pressed into point contact with the CSE, creating a small CSE-NW spacing, typically of order 10 μm. We measure the power spectral density (PSD) of the low-passed homodyne output to detect the corresponding Lorentzian response of NWs moving within close proximity of the CSE.[10]

Examples of a typical noise-driven voltage PSD and individual NW resonance lineshape are shown in Figure 2. The homodyne measurement technique detects both the motion of the PZT (correlated with applied drive voltage) and the resulting Lorentzian response of the NW. In Figure 2(a), the low-Q, broad resonance motion of the PZT is seen to carry on top of it the high-Q, narrow resonance peaks of NWs (indicated by stars). The combination of these two resonant motions—with an arbitrary relative phase—leads to the clear asymmetry seen in Figure 2(b). The red line in the figure fits the total PSD of the sum of a Lorentzian NW motion, a correlated PZT noise motion, and an additive and separately determined, uncorrelated, white noise arising from the front-end microwave amplifier. By comparison, we find that thermally driven noise peaks are entirely symmetric due to the lack of correlated noisy drive. The PSD in

a)Author to whom correspondence should be addressed. Electronic mail: Joshua.Montague@colorado.edu.
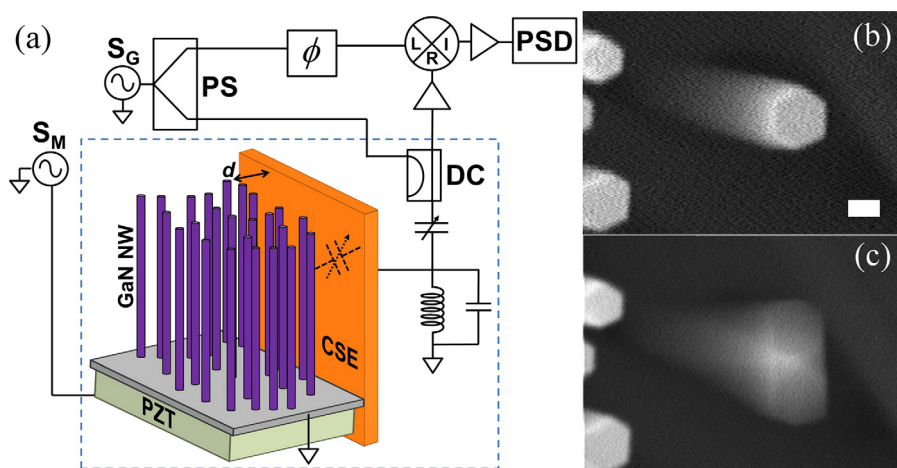
101, 173101-1

FIG. 1. (a) Schematic of the homodyne reflectometry system, comprising microwave ($\sim$3 GHz) signal source (S_G), power splitter (PS), phase adjustment (ϕ), mixer (L, R, I), directional coupler (DC), and PSD measurement. The microwave tone is injected into the cryostat (dashed, rectangular region) and coupled to the resonant circuit by a mechanically adjustable capacitance. The GaN NW sample is fixed atop a PZT (driven by source S_M) and aligned in close proximity to the CSE—typical separation $d \leq 10\,\mu$m. In our system, the CSE is a copper conductor in a microwave strip-line. At right: SEM micrographs illustrating (b) no PZT drive and stationary GaN NWs, and (c) same NWs while driving PZT at fundamental resonance frequency of central NW. The deflection of the NW causes a change in the NW to microwave resonator capacitance ((a), dashed) and allows detection of the NW motion via homodyne detection of the shift in microwave resonance frequency. Scale bar is 100 nm.

Figure 2(b) is displayed as NW deflection noise (nm²/Hz) and is calibrated by observation of thermally driven motion of the NW and application of the equipartition theorem.[11] This resonance peak was measured with a typical microwave power (for a 310 K measurement) of approximately 5 dBm incident on the resonant circuit.

Our reflectometry system is incorporated into a helium cryostat to allow variable temperature measurements of the as-grown NW ensembles. The sample temperature is read by a silicon diode sensor attached to the sample stage. Incident microwave power dissipated in the microwave tank circuit can cause sample heating. By reducing the microwave power incident on the reflectometer, we observe a microwave power threshold below which the diode thermometer is no longer affected at the 1-mK resolution of the temperature measurement. It is in this incident microwave power regime that we operate for each temperature. In the results below, the temperatures quoted are for the diode thermometer and represent an estimate of the minimum NW temperatures. In a typical experiment with GaN NWs on a substrate a few

square millimeters in size, it is common to observe 50 or more individual resonances well coupled to the microwave resonator, thus, allowing us to extract resonance frequencies and Q values for an ensemble of NWs (e.g., Figure 3). We have previously demonstrated that individual NWs in the ensemble can be simultaneously observed during mechanical vibration in an electron microscope (see Figure 1), thus, allowing us to connect specific NW resonance behavior with particular NW physical structure.[8]

Figure 3 shows a number of interesting ensemble behaviors. First, we note that the spread in mechanical resonance frequencies is well explained by an Euler-Bernoulli model for the NW resonance frequencies,[11] and the range of NW lengths and diameters separately observed by scanning electron microscopy.[10] Next, our data suggest the NW ensemble has a broader distribution in the observed NW resonance linewidths (and the associated Q values) than typical models for dissipation would ascribe due to processes with a characteristic damping rate and choice of NW vibrational frequency (see Eq. (1) below). Further, essentially independent
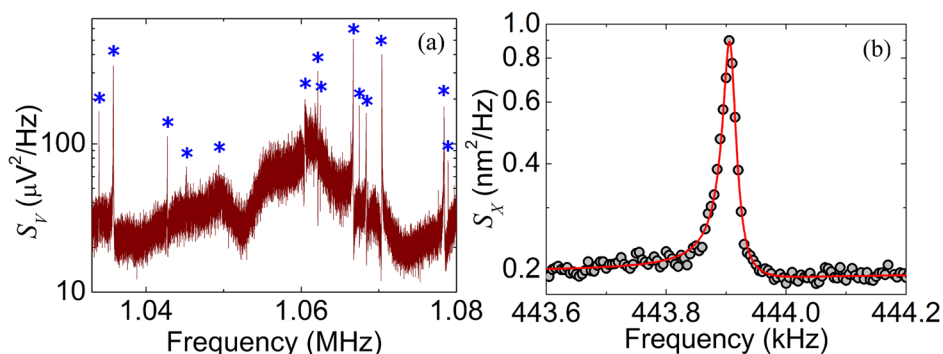

FIG. 2. PSDs of driven GaN NWs. (a) A $\sim$45 kHz portion of a voltage PSD, S_V, as detected by the homodyne reflectometry system. The GaN NW sample was driven by 1 Vrms white noise ($\leq$10 MHz) applied to the PZT. Individual GaN NW resonance peaks (blue stars) can be seen on top of very low-Q resonance motion from the PZT. (b) Displacement (S_x) PSD for a single, noise-driven (500 mV rms) NW resonance mode at 310 K. Solid red line is a fit to a Lorentzian line with a correlated noise from the PZT and an uncorrelated noise determined separately by an undriven spectrum, arising from the front-end amplifiers. The Lorentzian contribution to the data yields fitted parameters of $f_o = 443906.3 \pm 0.2$ Hz and $Q = 22200 \pm 400$. S_X is calibrated by measurement of a thermally driven resonance peak and application of the equipartition theorem. The integrated *rms* thermal deflection for this NW is roughly 6 Å.
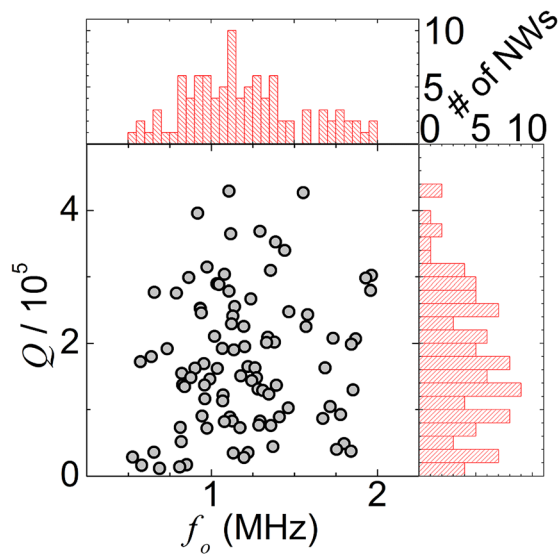
FIG. 3. Ensemble data and distribution of resonance frequencies and Q factors for 97 GaN NW resonances observed in a single measurement at 17 K. Top (side): histogram showing the range of resonance frequencies f_o (Q factors) with a bin size of 50 kHz (20 000).

of NW resonance frequency, we find that some NWs can have very low dissipation. For GaN NWs below 100 K, we regularly find Q values approaching 500 000 at the edge of the distribution.

Further information about the ensemble behavior can be extracted by considering the temperature-dependence of the resonance frequencies and Q factors. Figure 4 shows a subset of seven NWs from the full ensemble of Figure 3 (for visual clarity) whose temperature-dependent resonance frequency shifts span the observed range of the full ensemble. Such a shift in resonance frequency is consistent with stiffening due

to a temperature-dependent elastic modulus. A relative increase in resonance frequency of less than 1% over the range 12 K–320 K (relative to 300 K values) was observed for all NWs studied in this work. Near room temperature, the average measured frequency shift is 40 ± 20 ppm K^{-1}, consistent with previously reported results for GaN NWs,[4] yet too large to be explained by observed thermal expansion alone.[12] Similar behavior has been observed in silicon[13,14] and gallium arsenide[15] nanoscale resonators. We have fitted our data to a semi-empirical model of temperature-dependent elastic moduli previously used on silicon microresonators (the Wachtman equation):[13] $E(T) = E_o - BT \times \exp(-\Theta_D/2T)$, where E and E_o are, respectively, the temperature-dependent and zero-temperature Young's moduli, B is the bulk modulus, T is the temperature, and Θ_D is the Debye temperature. In the Figure 4 inset, we include a fit for a damped, cantilever beam resonance frequency with this temperature-dependent elastic modulus and fixed, bulk GaN values of Debye temperature and zero-temperature Young's modulus.

Interestingly, the ensemble data show a 20 ppm K^{-1} variation in the temperature-dependent relative resonance frequency shift at 300 K. We note that if all NWs in the ensemble shared the same thermal expansion coefficient and temperature-dependent Young's modulus, then all relative resonance frequency shifts should lie on the same curve. They clearly do not, indicating nanowire-to-nanowire variations in either or both of these quantities within the ensemble.

Figure 5 shows the dissipation Q^{-1} for the same 7 NW ensemble shown in Figure 4, with the same color- and symbol-coding. Near room temperature, typical values of Q^{-1} are near 10^{-4}. At slightly lower sample temperatures,
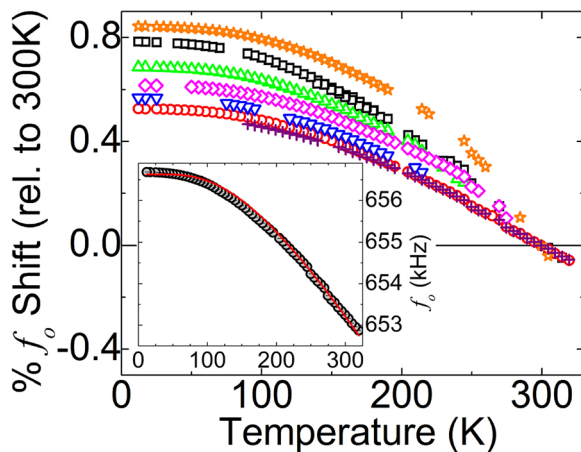

FIG. 4. Percent resonance frequency shifts for a seven-NW subset of the measured GaN NW ensemble, relative to their 300 K values. All measured NWs show less than 1% change over the range 12 K–320 K. Average frequency shift near 300 K is 40 ± 20 ppm K^{-1}. Room-temperature resonance frequencies are approximately: 573 kHz (black squares), 653 kHz (red circles), 733 kHz (green up-triangles), 1.12 MHz (blue down-triangles), 1.33 MHz (pink diamonds), 1.36 MHz (orange stars), and 2.44 MHz (purple crosses). The inset NW has a room-temperature resonance near 653 kHz. Solid red line is a fit to the data using an Euler-Bernoulli model for the resonance frequency with a temperature-dependent Young's modulus. Slight offsets in the single-NW data indicate temporal breaks in the experiment, where small amounts of adsorbed material likely modified resonance positions.
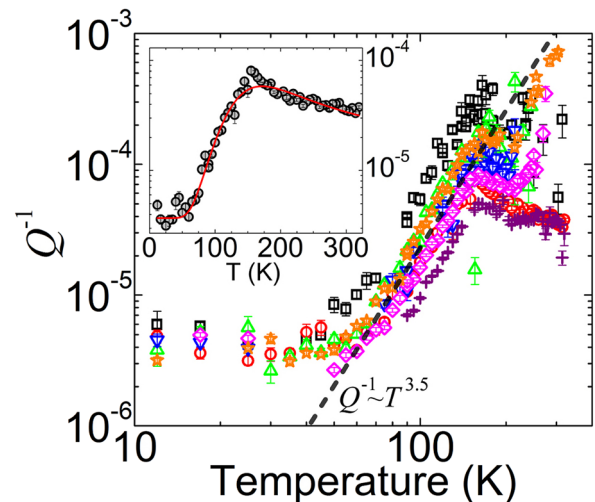

FIG. 5. Temperature dependence of GaN NW dissipation Q^{-1} for the seven-NW ensemble shown in Figure 4, with the same color- and symbol-coding. For all NWs studied, a dissipation peak is observed near 150 K, accompanied by a decrease in dissipation to a low-Q^{-1} plateau below 50 K. The single-NW shown (inset) is the same as the Figure 4 inset, and demonstrates similar behavior to the full ensemble. Solid red line is a fit to the data using the Debye equation and giving an activation energy $E_b \sim 70$ meV and attempt frequency $\tau_o^{-1} \sim 0.1$ GHz. The dashed line shows a $Q^{-1} \sim T^{3.5}$ approximation to guide the eye in the strongly temperature dependent region. Error bars are the results of nonlinear fitting to individual NW resonance peaks.

Q^{-1} remains approximately constant, though there is a weak maximum for all NWs near 150 K. Below this point, Q^{-1} decreases more quickly with temperature until roughly 50 K where it reaches what appears to be a low-dissipation plateau. The peak near 150 K and lower-temperature reduction of dissipation was typical of all NWs measured in this study. Below 100 K, we find that nearly all measured NW Q factors are near or above 10^5.

The general temperature dependence of NW dissipation is rather similar for the entire ensemble. In the region of 50 K–200 K, we observe that the loss Q^{-1} appears approximately proportional to $T^{3.5}$. This is a stronger power law dependence than that previously reported for dissipation in nanostructure resonators composed of silicon carbide[16] (temperature exponent = 0.3), nanocrystalline diamond[17] (0.2), gold[18] (0.5), carbon nanotubes and graphene[19] (0.36), and silicon[20] (0.36). Figure 6 illustrates that there is a correlation between greater relative resonance frequency shifts near room temperature and greater dissipation observed near a 150 K loss peak. This same correlation persists at all the temperatures we have investigated. We also observe variations in the dissipation for NWs of roughly equal relative frequency shift.

In an attempt to understand the measured dissipation in these NWs, we have compared the results to standard loss mechanisms of the form:[21–24]

$$Q^{-1}(\omega) \propto \Delta_i(T) \frac{\omega \tau_i}{1 + (\omega \tau_i)^2}. \qquad (1)$$

In Zener's thermoelastic damping (TED) model, the "relaxation strength" is $\Delta_{TED} = E\alpha^2 T/C_p$ and $\tau_{TED} = d^2/(\pi^2\chi)$. In these equations, E is the Young's modulus, α is the linear thermal expansion coefficient, T is the temperature, C_p is the heat capacity at constant pressure, d is the resonator beam width, and χ is the thermal diffusivity. Thermoelastic damping predicts the type of correlation we observe between temperature-dependent Young's modulus and dissipation.

However, with standard GaN material properties,[12] this model also puts a lower bound on Q^{-1} of order 10^{-6} at 300 K, and 10^{-9} near 50 K, for these measured frequencies; both much lower than our measured values. The model also would not explain the variations we observe in dissipation of NWs of nominally equal temperature-dependent Young's modulus. The exact formulation of Zener's approximation by Lifshitz *et al.*[24] yields nearly identical results.

In a typical model of thermally activated defect motion,[25] Δ_{def} is a similarly dimensionless percent change in the modulus (between relaxed and unrelaxed states), and τ_{def} obeys an Arrhenius equation $\tau_{def} = \tau_o \times \exp[E_b/(k_B T)]$, where τ_o^{-1} is an attempt frequency and E_b the associated activation energy (or barrier height). Assuming Δ_{def} is independent of temperature, a fit to our Q^{-1} data with a single such "Debye peak" (Figure 5 inset) consistently results in activation energies of order of 0.1 eV and attempt frequencies of order 1 GHz. Though the energy scale is reasonable for point defects or surface species of a solid, the attempt frequencies are substantially lower than the typical 1 THz expected for solids.[26] It is worth noting that measured wurtzite GaN phonon modes[27] and calculated *m*-plane Ga adatom kinetics[28] have both been reported in this energy region. Additionally, previous studies have indicated a maximum in electron mobility in the vicinity of 140 K.[29,30] Further experiments will be required before the dissipation mechanism is firmly identified.

In summary, we report on the temperature-dependent mechanical resonance properties of as-grown, *c*-axis GaN NW ensembles. Our measurements make use of a flexible and simple, capacitively coupled, homodyne reflectometry measurement system compatible with cryogenic measurements. Measured resonance frequencies demonstrate temperature dependence consistent with a stiffening elastic modulus, with unique variations within the ensemble. Measured dissipation demonstrates a rapid reduction below 150 K and appears to reach a plateau in the vicinity of 50 K with Q values typically well above 10^5. The ability to measure ensemble properties is critical in revealing and correlating variations in the unique nanowire properties. Further ensemble measurements should help us understand the origin of these very high Q values, and will improve our understanding of the mechanisms behind the observed dissipation. The ensemble readout should find application both in fundamental studies, such as those reported here, and in nanowire-based sensor applications.
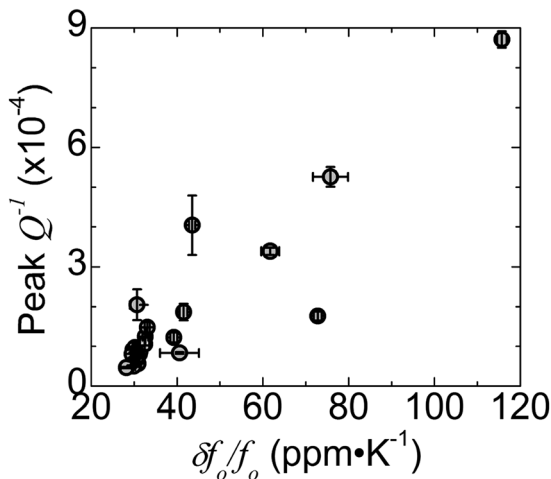
FIG. 6. Variations in peak dissipation Q^{-1} in the region near 150 K appear to be correlated with relative resonance frequency shifts near room temperature. Shown are the 25 GaN NW resonances with sufficient measurement data at both temperatures. Error bars are the results of nonlinear fitting to individual NW resonance peaks.

[1]J. D. Teufel, T. Donner, M. A. Castellanos-Beltran, J. W. Harlow, and K. W. Lehnert, Nat. Nanotechnol. **4**, 820–823 (2009).

[2]H. J. Mamin and D. Rugar, Appl. Phys. Lett. **79**, 3358 (2001).

[3]K. L. Ekinci, X. M. H. Huang, and M. L. Roukes, Appl. Phys. Lett. **84**, 4469 (2004).

[4]S. M. Tanner, J. M. Gray, C. T. Rogers, K. A. Bertness, and N. A. Sanford, Appl. Phys. Lett. **91**, 203117 (2007).

[5]K. A. Bertness, N. A. Sanford, and A. V. Davydov, IEEE J. Sel. Top. Quantum Electron. **17**, 847–858 (2011).

[6]K. A. Bertness, A. Roshko, L. M. Mansfield, T. E. Harvey, and N. A. Sanford, J. Cryst. Growth **310**, 3154–3158 (2008).

[7]J. R. Montague, M. Dalberth, J. M. Gray, D. Seghete, K. A. Bertness, S. M. George, V. M. Bright, C. T. Rogers, and N. A. Sanford, Sens. Actuators, A **165**, 59–65 (2011).

[8]J. M. Gray, C. T. Rogers, K. A. Bertness, and N. A. Sanford, J. Vac. Sci. Technol. B **29**, 052001 (2011).

[9]S. W. Hoch, J. R. Montague, V. M. Bright, C. T. Rogers, K. A. Bertness, J. D. Teufel, and K. W. Lehnert, Appl. Phys. Lett. **99**, 053101 (2011).

[10]J. Montague, K. Bertness, N. Sanford, V. M. Bright, and C. T. Rogers, in Proceedings of ASME 2011 International Mechanical Engineering Conference and Exposition, Denver, CO, 2011.

[11]A. N. Cleland, *Foundations of Nanomechanics: From Solid-State Theory to Device Applications* (Springer-Verlag, Berlin, 2003).

[12]M. E. Levinshtein, S. L. Rumyantsev, and M. S. Shur, *Properties of Advanced Semiconductor Materials: GaN, AIN, InN, BN, SiC, SiGe* (John Wiley & Sons, Hoboken, 2001).

[13]U. Gysin, S. Rast, P. Ruff, E. Meyer, D. Lee, P. Vettiger, and C. Gerber, Phys. Rev. B **69**, 045403 (2004).

[14]S. Evoy, A. Olkhovets, L. Sekaric, J. M. Parpia, H. G. Craighead, and D. W. Carr, Appl. Phys. Lett. **77**, 2397 (2000).

[15]P. Mohanty, D. Harrington, K. Ekinci, Y. Yang, M. Murphy, and M. Roukes, Phys. Rev. B **66**, 085416 (2002).

[16]X. L. Feng, C. A. Zorman, M. Mehregany, and M. L. Roukes, in Solid-State Sensors, Actuators and Microsystems Workshop (Hilton Head 2006) (Hilton Head Island, SC, 2006), pp. 86–89.

[17]A. B. Hutchinson, P. A. Truitt, K. C. Schwab, L. Sekaric, J. M. Parpia, H. G. Craighead, and J. E. Butler, Appl. Phys. Lett. **84**, 972 (2004).

[18]A. Venkatesan, K. J. Lulla, M. J. Patton, A. D. Armour, C. J. Mellor, and J. R. Owers-Bradley, J. Low Temp. Phys. **158**, 685–691 (2009).

[19]C. Chen, S. Rosenblatt, K. I. Bolotin, W. Kalb, P. Kim, I. Kymissis, H. L. Stormer, T. F. Heinz, and J. Hone, Nat. Nanotechnol. **4**, 861–867 (2009).

[20]G. Zolfagharkhani, A. Gaidarzhy, S.-B. Shim, R. Badzey, and P. Mohanty, Phys. Rev. B **72**, 224101 (2005).

[21]C. Zener, Phys. Rev. **52**, 230–235 (1937).

[22]C. Zener, Phys. Rev. **53**, 90–99 (1938).

[23]C. Zener, W. Otis, and R. Nuckolls, Phys. Rev. **53**, 100–101 (1938).

[24]R. Lifshitz and M. Roukes, Phys. Rev. B **61**, 5600–5609 (2000).

[25]A. S. Nowick and B. S. Berry, *Anelastic Relaxation in Crystalline Solids* (Academic, New York, 1972).

[26]A. N. Cleland and M. L. Roukes, J. Appl. Phys. **92**, 2758 (2002).

[27]D. Manchon, Solid State Commun. **8**, 1227–1231 (1970).

[28]L. Lymperakis and J. Neugebauer, Phys. Rev. B **79**, 241308(R) (2009).

[29]D. C. Look, J. R. Sizelove, S. Keller, Y. F. Wu, U. K. Mishra, and S. P. DenBaars, Solid State Commun. **102**, 297–300 (1997).

[30]A. F. M. Anwar and R. T. Webster, IEEE Trans. Electron Devices **48**, 567–572 (2001).